

## Green Synthesis of Tupi Nanas Leaves Waste Silver Nanoparticles

Devesh Pravinkumar Bhavsar<sup>1</sup>, Sai Koteswar Sarma<sup>2</sup>, Priyanjali Biswas<sup>3</sup>, Omsatyam<sup>4</sup>,  
Ashruti Hor<sup>5</sup>, Rajeev Ranjan<sup>6</sup>, Nihar Ranjan Kar<sup>7</sup>, Sushilkumar Ananda Shinde<sup>8</sup>,  
Dipansu Sahu\*

1. *Asst.Professor, KES's Late Shri P.C.Bhandarkar College of D. Pharmacy & Late Shri Prof R.K.kele College of B.Pharmacy, Amalner. Dist-Jalgaon, Pin Code:425401*
2. *Professor, Department of Pharmacognosy, Sri Padmavathi School of Pharmacy, Tiruchanoor, Tirupati, Andhra Pradesh affiliated to JNTUA, Pin Code:517 503*
3. *Research Scholar, NIMS University, NH-11C, Delhi-Jaipur Expy, Shobha Nagar, Jaipur, Rajasthan, Pin Code:303121*
4. *Assistant Professor, Narayan Institute of Pharmacy, Gopal Narayan Singh University, Jamuhar, Sasaram, Bihar, Pin Code: 821305*
5. *Assistant Professor, Netaji Subhash University Pokhari, PO: Bhilai Pahari, PS: MGM, Dist:, Jamshedpur, Jharkhand, Pin Code: 831012*
6. *Assistant Professor, Univ. Department of Chemistry, DSPM University, Ranchi, Pin Code: 834008*
7. *Assistant Professor, Centurion University of Technology and Management, Gopalpur, Balasore, Odisha, India, Pin Code:756044*
8. *Associate Professor, PRMSS Anuradha College of Pharmacy Chikhli Anuradha Nagar Sakegaon Road, Chikhli, Pin Code: 443204*

**Corresponding author:** Dipansu Sahu

tuludipansu@gmail.com

**Affiliation:** Associate Professor, Shree Naranjibhai Lalbhai Patel College of Pharmacy,  
UmraKh Bardoli Surat Gujarat

---

### Abstract

Present is a low-cost and environmentally beneficial approach for producing silver nanoparticles from discarded pineapple leaves utilising microwave-assisted extraction. AgNPs are produced environmentally friendly using a straightforward reduction technique and silver nitrate. The ideal conditions for green synthesis are determined by taking into account a number of factors, such as the silver nitrate concentration (5–25 mM), the incubation period (2–24 h), and the sample volume (2–8 mL). The reduction of silver metal ions into silver nanoparticles is indicated by the appearance of an absorption band in the UV-Vis spectro-photometer between 400 and 500 nm. Longer run times, higher silver nitrate solution concentrations, and larger sample volumes are all observed to improve absorption intensity. The green synthesised silver nanoparticles range in size from 40 to 150 nm and exhibit hexagonal spherical shapes, according to FE-SEM studies. Furthermore, the presence of green synthesised AgNPs is confirmed by FTIR and XRD studies. In comparison to non-microwave-assisted treatment, silver nanoparticles treated with a microwave show increased antibacterial activity against *Escherichia coli*, *Bacillus subtilis*, and *Staphylococcus aureus*. Silver nanoparticles must be present at a minimum of 60 g/mL to

suppress bacterial growth. Overall, this study provides an avenue with substantial potential for the environmentally friendly and economically advantageous green synthesis of silver nanoparticles employing the microwave-assisted technique.

**Keywords:** AgNPs, Silver nanoparticles, *Staphylococcus aureus*, Tupi Nanas Leaves

---

## Introduction

Nanotechnology is a cutting-edge scientific field with many applications in a variety of areas, including energy, manufacturing, and biological research. Nanotechnology makes it feasible to use novel methods in biomedical research that were previously impractical by creating nanoparticles (NPs) with distinctive compositions and capabilities. It is impossible to ignore the many potentials, benefits, and uses of nanotechnology in biology and biomedical research. Since they have recently been discovered to exhibit potent inhibitory and antibacterial properties, silver nanoparticles (AgNPs) have become a hot issue in a variety of industries, including biomedical device coatings, food packaging, cosmetics, water purification, and even as medicinal agents. Due to their special electrical, optical, and magnetic characteristics that have a wide range of applications, AgNPs, which range in size from 1 to 100 nm, have garnered attention<sup>1</sup>. AgNPs can also lessen bacterial infections in wounds and on the skin, as well as prevent bacterial colonisation on various device surfaces. AgNPs can be made physically or chemically, but both of these procedures are expensive and raise environmental concerns because they use hazardous chemicals and produce dangerous byproducts. The advantage of using a green synthesis method to make AgNPs is that it reduces possible dangers associated with using conventional chemical or physical synthesis techniques. As a result, it plays a significant role in assuring the safety and sustainability of AgNPs' use in a variety of domains. In response to this worry, techniques for making colloidal AgNPs that are both safe and environmentally friendly have been devised, such as using plants or microorganisms<sup>2</sup>. Due to its benefits over microbes, which require an aseptic environment for cell growth, such as being non-toxic, environmentally friendly, and economical, plant-mediated synthesis is increasingly becoming a preferred method. Plants act as capping and reducing agents for the synthesis of AgNP because they are rich in biomolecule components such as proteins, flavonoids, polyphenols, and other phytochemicals. The resultant particles have a range of sizes and shapes and are stable<sup>3</sup>. Furthermore, microwave-assisted green synthesis of AgNPs is significant since it has been shown to have numerous benefits in a variety of disciplines and is easily adaptable to varying size and structural requirements. *Aegle marmelos*, *Pteris tripartite*, *Prosopis farcta*, *Acalypha indica*, *Curcuma longa*, *Ananas comosus*, and many other species have been utilised to make AgNP. Along with papaya, pomelo, banana, watermelon, jackfruit, and mango, *A. comosus*, or pineapple, is one of the most important fruits grown in Malaysia<sup>4</sup>. As much as 30 to 50 percent of the weight of the entire fruit is lost during canning, which accounts for a major portion of the waste produced during pineapple processing, which also includes stems, crowns, cores, and peels. Currently, Malaysia produces 95% of its canned pineapple for export and 5% for internal use. To limit the amount of waste, a waste-to-wealth project has been put forth to transform this waste into something beneficial. The waste from MD2 "Super Sweet"

pineapple leaves can operate as a capping and reducing agent for the green synthesis of AgNPs utilising a microwave-assisted process, and this work demonstrates that it has the potential for antibacterial applications in a variety of domains. The unique aspect of this work is the use of a microwave-assisted approach, which uses less energy than a conventional heating method to convert Ag<sup>+</sup> ions to Ag<sup>0</sup> in place of that method. In terms of energy consumption, this novel technique offers advantages that are more environmentally friendly and time-effective<sup>5</sup>.

### **Methodology**

#### **Materials**

From On Silica Gel, iPlatinum Pvt. Ltd silver nitrate (AgNO<sub>3</sub>) was purchased. Waste pineapple leaves from the pineapple plantation sector were gathered.

#### **Preparation of pineapple leaf waste extract**

To remove dust, the wasted pineapple leaves are properly washed under running water several times, and then rinsed with distilled water. The leaves are broken up into little bits and weighed at about 100 g. These leaves are then cooked for 30 minutes at 100 degrees in 400 mL of purified water before being strained. A portion of the filtrate is utilised in the green synthesis of AgNPs as a stabiliser and reducing agent. In order to protect the aqueous plant extract from contamination, the filtrate is kept at 20°C. The filtrate's remaining leaves are dried in an oven to a consistent weight before being combined as a control for FTIR analysis<sup>6</sup>.

#### **AgNPs Green synthesis**

The green synthesis of AgNPs is performed using aqueous extraction from wasted pineapple leaves through a simple reduction method with AgNO<sub>3</sub>. The green synthesis process is done in accordance to Kumar et al. (2021) with slight modifications. To begin, 20 mM of AgNO<sub>3</sub> solution is added to 4 mL of the pineapple leaves extract solution in a total volume of 20 mL, with stirring. The solution is then incubated at room temperature<sup>7</sup>. The green synthesis is conducted by comparing microwave-assisted treatment with normal condition. The microwave-assisted treatment is performed at a constant power of 10% x 1100 Watts for 9 min. Upon completion, the colour of aqueous extract changes from colourless to reddish brown slowly when adding AgNO<sub>3</sub>. The rapid formation of a reddish-brown solution, as shown in Figure:1, indicates the successful formation of AgNPs through the reduction of silver ions in the solution. The green synthesized AgNPs are then purified by washing twice with distilled water, centrifuging (using MPW-352R, Germany) at 8000 rpm for 10 min, and lyophilizing using a freeze drier machine. Different parameters include AgNO<sub>3</sub> concentration (5–25 mM), incubation time (2–24 h) and sample volume (2–8 mL) are further studied to determine the optimal condition for synthesizing AgNPs<sup>8</sup>.

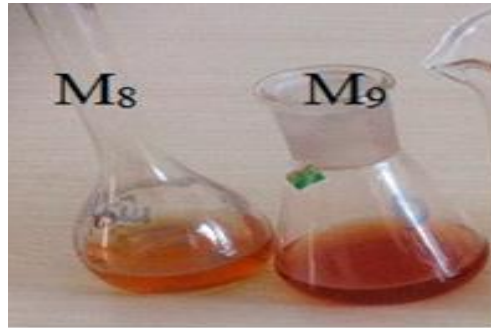


**Figure No 1:-** Aqueous solution's colour under microwave assistance

(a) before adding AgNO<sub>3</sub> and (b) after adding AgNO<sub>3</sub>. (The reader is directed to the Web version of this article for interpretation of the references to colour in this figure legend.)

### **AgNPs Silver Nano-particles Characterization**

#### **UV-visible spectrophotometer**

AgNPs silver green synthesized silver nano particles, which entail the reduction of pure silver ions, are initially characterised using the UV-visible microplate spectrophotometer reader (Epoch microplate spectrophotometer, US). In the wave length range of 350 to 600 nm, the surface plasmon absorption is observed<sup>9</sup>.

#### **Field-Emission Scanning Electron Microscopy (FESEM)**

The prepared gold coated samples are characterized under FESEM (ZEISS, Crossbeam 340, Germany) to observe the morphological characterization of green synthesized AgNPs<sup>10</sup>.

#### **Fourier Transform Infrared (FTIR)**

Using an FTIR spectrophotometer (Perkin-Elmer Spectrum One FT-IR Spectrometer, USA) with a range of 4,000 to 400 cm<sup>-1</sup>, the leaves left over after extraction and the green synthesised AgNPs are examined<sup>11</sup>.

#### **X-Ray Diffractometer (XRD)**

On the powdered AgNP samples, X-ray diffraction (XRD) is carried out using a Japanese Shimadzu XRD-6000 apparatus. By drop-coating the AgNPs onto glass substrates, their size is calculated, and their presence is verified by analysing the dried mixture after the water has evaporated at room temperature. With a voltage of 40 kV and a current of 30 mA, Cu K radiation is used to conduct the XRD analysis in a "to 2" configuration<sup>12</sup>.

#### **Antimicrobial activity**

##### **Microbial culture**

In total, three bacteria were taken from ATCC 6538. Gram-positive *B. subtilis* and *S. aureus* and Gram-negative *E. coli* were among the bacterial strains. *S. aureus* is designated as the most prevalent infection bacterium in wounds<sup>13</sup>.

##### **Disk diffusion antibacterial assay**

According to Baskaran et al. (2016), a disc diffusion antimicrobial assay was performed. A sterile Petri dish is used to create agar plates by adding 20 mL of nutritional agar liquid, which is then covered with 0.1 mL of bacterial suspension after it has solidified. 6 mm diameter sterile filter paper discs were impregnated with 5 and 10 L of 5 mg/mL AgNPs, and the plates were

then incubated at 37°C for 24 hours. By assessing the zones of inhibition against the test microorganisms, antibacterial activity was measured<sup>14</sup>.

### **Broth antibacterial assay**

Meanwhile, 15 mL of nutritional broth (NB) containing varying concentrations of green synthesised AgNPs is added to 1 mL of three types of bacterial suspension in nutrient broth (NB). For 24 hours, the bacterial suspensions are incubated. A spectrophotometer (UV-1280 spectrophotometer, Shimadzu, Japan) optical density (OD) reading at 600 nm is used to calculate the dry cell weight to calculate the bacterial growth after 24 hours<sup>15</sup>.

## **Results and discussion**

### **Optimal condition for green synthesis of AgNPs**

In comparison to previous approaches, the green synthesis of AgNPs utilising waste pineapple leaf extract has the potential to be more favourable because it is simple to modify, less biohazardous, and chemically toxic-free. Additionally, it offers organic capping agents for the stabilisation of silver nanoparticles and is less expensive than microorganism-based nanoparticle manufacturing. Wasted pineapple leaves are collected, thoroughly washed under running water (necrotic plants and epiphytes were removed), then washed once more in sterile distilled water (associated debris were removed). Next, the leaves are cut into small pieces, boiled in distilled water, and the extract is filtered<sup>16</sup>. A part of the filtrate from the boiled and filtered pineapple leaf extract is used as a reducing agent and stabiliser during the production of AgNPs. When AgNO<sub>3</sub> solution was added to a small amount of plant extract under standard or microwave-assisted treatment conditions, a reaction took place. In this work, a number of parameters were examined, and the conversion of pure Ag (I) ions to Ag(0) was tracked by measuring the solution under a UV-vis spectrophotometer microplate reader at regular intervals<sup>17</sup>.

### **AgNO<sub>3</sub> different concentration's Effect**

To identify the ideal concentration of AgNO<sub>3</sub> to lower the silver ion for green synthesised AgNPs in 4 mL leaves extract solution, the effects of various AgNO<sub>3</sub> concentrations (range from 5 to 25 mM) are investigated. The greatest peak ranges between 400 and 450 nm at various doses of AgNO<sub>3</sub> during green synthesis of AgNPs during 2 h incubation period are exhibited in UV-vis spectrophotometry micro plate reader in Fig. 2. Both Mojally et al. (2022) and Lade and Patil (2022) showed similar UV spectrum ranges using aqueous mint extract and *Passiflora foetida* Linn leaf extract, respectively. The Surface Plasmon Resonance (SPR) band is produced by the collective oscillations of conduction electrons in nanoparticles in the presence of visible light, and it is greatly influenced by the size and form of the nanoparticles<sup>18</sup>. When the AgNPs made from the pineapple leaf extract were hung in water, they had a reddish-brown colour. This is because the reduction of Ag<sup>+</sup> into Ag<sup>0</sup> excited electrons and changed the electronic energy levels (Emeka et al., 2014). According to Fig. 2a, the green synthesis performs better with higher peaks at 20 mM of AgNO<sub>3</sub> for two hours when treated with a microwave<sup>19</sup>. This suggests that, compared to other concentrations, a concentration of 20 mM AgNO<sub>3</sub> is adequate to diminish the silver ion in green synthesised AgNPs. As concentration rises due to an increase in the absorption of organic chemicals, the band around 400–450 becomes more intense (Ramya,

2021). The SPR intensity decreases as the concentration rises to 25 mM, though. This phenomenon might be caused by the limited ability of active functional groups to serve as reducing agents in the extract of pomelo peels. In contrast, no discernible difference can be seen in the usual situation (Fig. 2b), where a slower reaction to the reduction of the silver ion takes place without microwave treatment<sup>20</sup>.

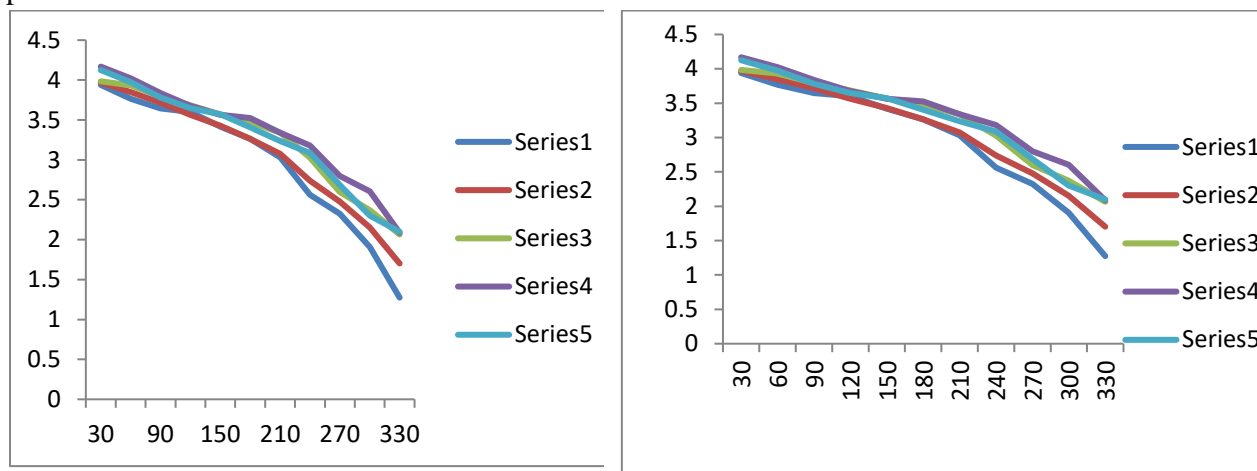
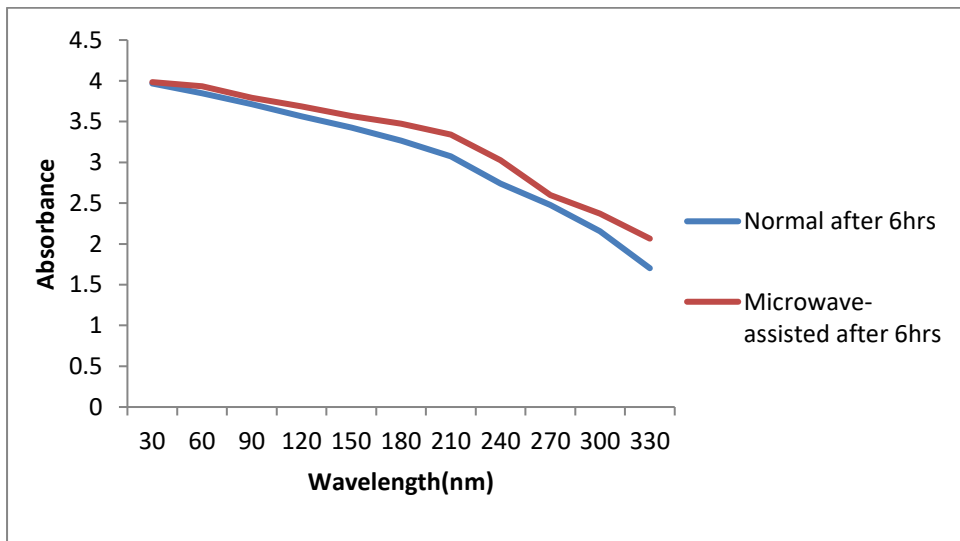
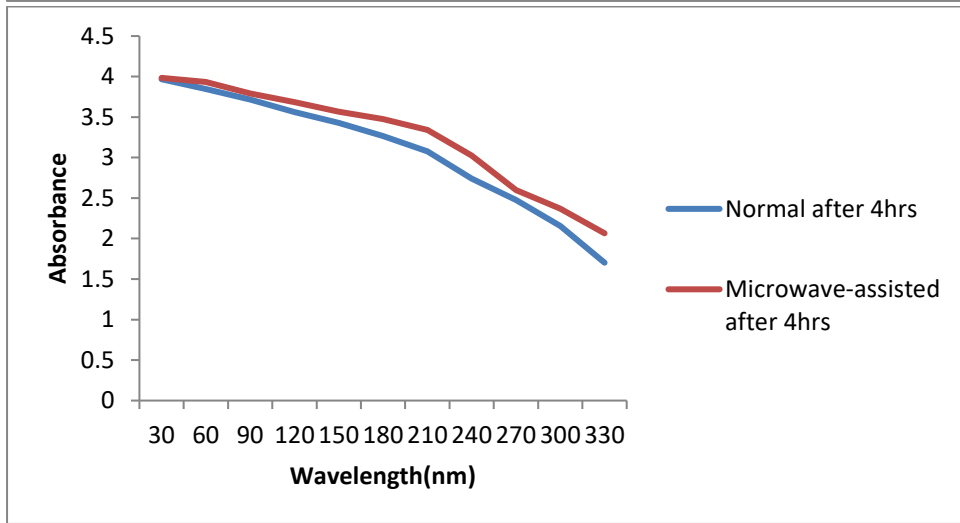
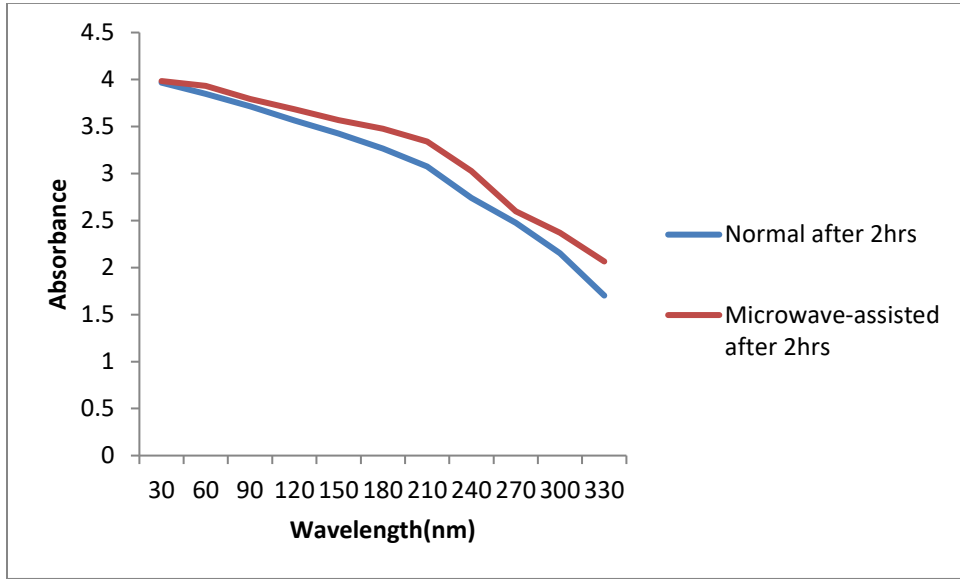


**Figure No 2:-** Effect of different AgNO<sub>3</sub> concentration on green synthesized AgNPs for  
(a) Microwave-assisted treatment;

(b) Normal condition. (For interpretation of the references to colour in this figure legend, the reader is referred to the Web version of this article.)

### Effect of different incubation time

The effect of different incubation time (2, 4, 6, 24 h of incubation) on green synthesized AgNPs with normal condition and microwave-assisted treatment at 20 mM AgNO<sub>3</sub> and 4 mL extract leaves is examined as shown in Fig. 3. The intensity UV–Vis spectra of the absorption increase with distinctive plasmon band ranging between 400 and 450 nm with prolong time incubation, indicating the formation of the AgNPs increased by continuous incubation until 24 h. During the initial incubation, the SPR peak was observed at approximately 401 nm, which gradually shifted towards longer wavelengths with the increase in reaction time<sup>21</sup>. The intensity of the SPR peak was observed to increase with an increase in reaction time, suggesting a higher concentration of the synthesized AgNPs. The enhancement in SPR intensity could potentially be attributed to the conversion of hydroxyl (OH) groups to carbonyl (C=O) groups as a result of the reduction of silver ions, as suggested by Jalani et al. (2018). Fig. 3e depicts the comparison of green synthesis AgNPs by normal condition with microwave-assisted treatment with different incubation time at 425 nm. Green synthesis of AgNPs by microwave-assisted treatment accelerates more formation of AgNPs during 2–6 h of incubation as compared with green synthesis in normal condition. The formation of AgNPs achieves same intensity after 24 h of incubation and the graph intensity becomes flatter, representing a completion of AgNPs formation in the reaction suspension<sup>22</sup>.



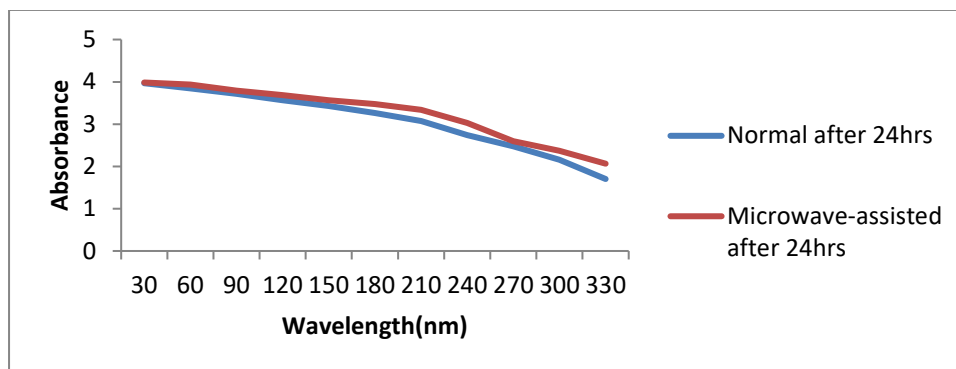


**Figure No 3:-** Effect of different incubation time on green synthesized AgNPs under (a) 2hr; (b) 4 h; (c) 6 h (d) 24 h of incubation time

### Effect of different sample volume

Different sample volumes (2, 4, 6, 8 mL) of extracted wasted pineapple leaves are employed in green synthesis under 6 h incubation. The peaks are observed in the range of 400–450 nm as shown in Fig. 4 for both experiment with and without microwave-assisted treatment. Both results reveal that 6 mL and 8 mL sample volume of leaves extract are sufficient for the reaction with 20 mM AgNO<sub>3</sub>. This is because the highest wavelength was performed by 6 mL and 8 mL, indicating faster reduction activity of silver ion<sup>23</sup>. It is in line with the study done by Jyothi et al. (2022) where 8 mL of *Spondias pinnata* bark extract was the optimal amount of AgNPs synthesis by microwave irradiation as the SPR band changed with different volume. Therefore, AgNPs synthesized from the treatment of 20 mM of AgNO<sub>3</sub> using 6 mL sample volume with microwave-assisted treatment for 6 h of incubation time was employed for further characterization analysis<sup>24</sup>.

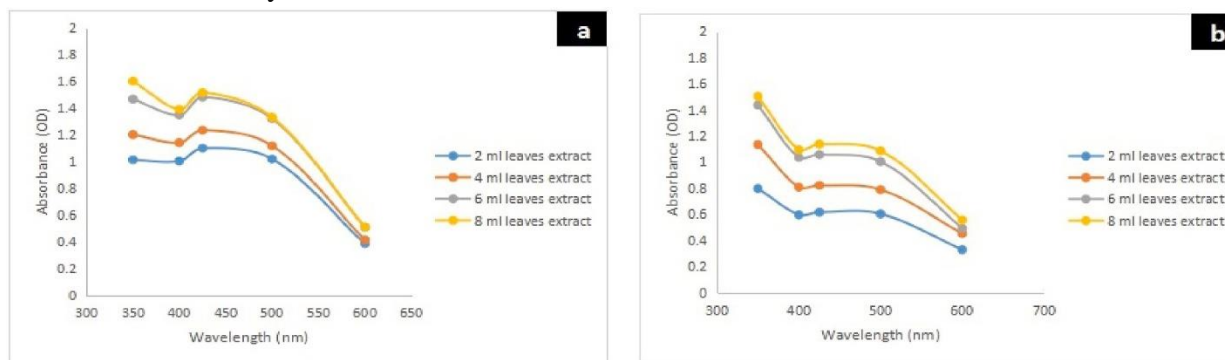


**Figure 4.** Effect of different sample volume of extraction wasted pineapple leaves for (a) Microwave-assisted treatment; (b) Normal condition.

### Particle size and morphology

Figure no 5 illustrates the morphology and particle size of AgNPs synthesized using microwave-assisted method<sup>25</sup>. The nanoparticles are observed to have a hexagonal spherical shape, with a size range between 40 and 150 nm. The size of AgNPs is slightly larger than that in the work by Maryani and Septama (2022) ( $21.63 \pm 4.85$  nm) and Jyothi et al. (2022) (34.52 nm). Researchers



claimed that smaller size could perform better antimicrobial activity since it can penetrate to bacterial cells easily thereby disrupting their cell wall. Moreover, spherical size of AgNPs demonstrates a larger specific surface area compared to nanorods and nanowires (Acharya et al., 2018) thus can inhibit the antimicrobial growth more effectively through penetration and reaction with bacterial cell wall<sup>26</sup>.

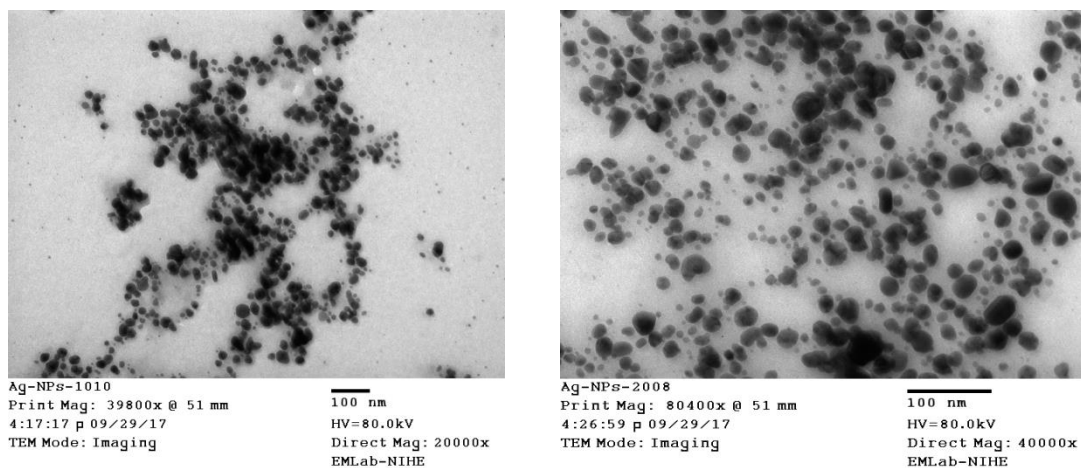


**Figure No 5:** Particle size of silver nanoparticles

#### **Fourier Transform Infrared Spectroscopy (FTIR) analysis**

Functional groups in samples can be examined with FTIR spectroscopy in order to verify the efficacy of each step of the treatment. Fig. 6 depicts FTIR spectra of pineapple leaves; A - pineapple leaves extract and B - AgNPs. The comparison study is conducted to observe any changes in chemical bond of pineapple leaves after the synthesizing process. Pineapple leaves extract contain numerous bioactive compounds such as glycosides, proteins, phenolics, flavonoids, tannins, and terpenoids<sup>27</sup>. Flavonoids are crucial compounds that act as reducing agents during the synthesis of AgNPs among these compounds. To identify the functional groups that are responsible for capping and stabilizing the Ag nanoparticles, FTIR analysis was performed in the range of 600–4000  $\text{cm}^{-1}$ . The FTIR spectrum of both sample (A - pineapple leaves extract and B - AgNPs) showed four different peaks in Figure No 6. The stretching intensity shown in the graph of synthesized leaves decreases and becomes broader compare to the control because of the removal of impurities such as hemicellulose and lignin removal. The shifting of peaks between pineapple leaves extract which may suggest the involvement of the functional group in the formation of AgNPs<sup>28</sup>. The presence of hydrogen-bonded hydroxyl (–OH) group compounds was indicated by the broad band at 3,729  $\text{cm}^{-1}$  (A) which shifted to 3,735  $\text{cm}^{-1}$  (B). The highest energy region of the spectrum, known as the “hydrogen region”, ranges from 3,800 to 2,700  $\text{cm}^{-1}$ . The observed peak at 1,610  $\text{cm}^{-1}$  (A) which shifted to 1,628  $\text{cm}^{-1}$  (B) indicated the presence of C=O stretching bonds of the carbonyl group. Amino acid residues containing carbonyl groups can form a strong bond with metals. Proteins with these residues may create a coating that covers the metal nanoparticles, preventing them from agglomerating in solution. The ligands capping the AgNPs may contain an aromatic compound, C=C of alkenes,

or C=N amine stretching, as indicated by previous studies<sup>29</sup>. The wide absorption spectra at  $1,036\text{ cm}^{-1}$  (A) was due to the stretch vibrations of C-N stretching and C-O stretching of amino and carboxyl groups which mainly attributed from flavonoids and terpenoids in pineapple leaves extract. Then, the reducing of these peaks at  $1042\text{ cm}^{-1}$  (B) suggested the involvement of these bioactive compounds in reducing silver ions to AgNPs (Jalani et al., 2018). Therefore, the obtained FTIR spectra provided evidence for the production of AgNPs through the reduction of  $\text{Ag}^+$  ions by the capping material present in the aqueous leaves extract<sup>30</sup>.

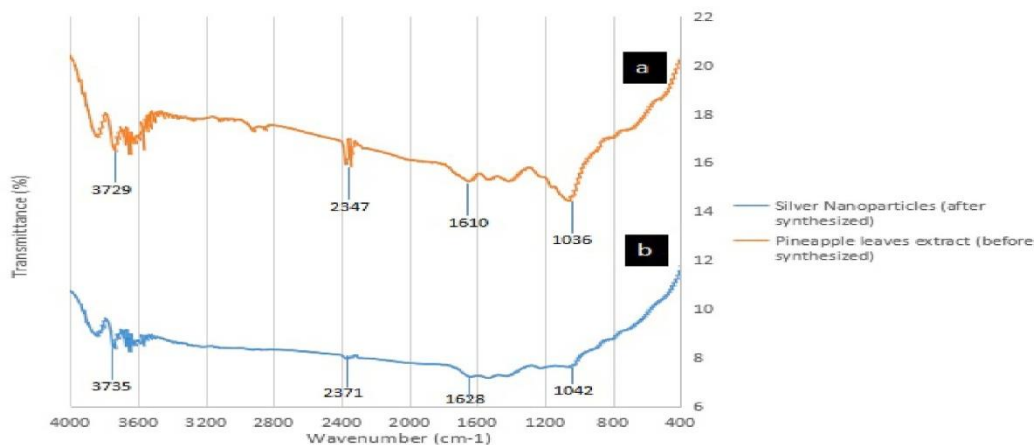


**Figure No 6:** FTIR absorbance spectra of control (residual leaves filtrated), A-leaves extract (before synthesized) and B- AgNPs (after synthesized)

### X-Ray diffraction (XRD) analysis

The crystalline phase of the presence and absence of AgNPs sample is analyzed in the range of  $2\theta$  between  $10^\circ$  and  $100^\circ$ . As illustrated in Figure no 7, the sample has crystalline structures and three main characteristic peaks at  $27.6^\circ$ ,  $32^\circ$  and  $46^\circ$  which are attributed to crystallographic planes at 111, 200 and 220 (crystalline region). These are the crystal reflection planes of the face-centered cubic (fcc) lattice of silver respect to the standard data (Joint Committee on Powder Diffraction Standard data No 04-0783), confirming that the AgNP was successfully green synthesized from wasted pineapple leaves with microwave-assisted treatment. This is validated by previous study as the characteristic peaks were indistinguishable from the biosynthesis of AgNPs from apple pomace and aqueous *Desmodium triquetrum* extract (Maryani and Septama, 2022). The observed peaks in this study are also intense and sharp, indicating a high degree of crystallinity of green synthesized AgNPs. Similar patterns are observed for AgNPs synthesized from fern, *Pteris tripartite* Sw. (Baskaran et al., 2016) which showed three intense peaks between  $20^\circ$  and  $50^\circ$ . In comparison of the intensity ratio, crystallographic plane at 200 has the highest intensity. This could be inferred that green synthesized AgNPs is enriched in (200) facets thereby this plane exhibits a preference to align parallel to the surface of the substrate it is supported on, followed by planes at 220 and 111. The crystallite size of AgNPs is calculated using Debye-Scherrer's formula<sup>31</sup>:

$$D = 0.94 \lambda / \beta \cos \theta$$

where  $D$  denotes the average crystalline domain size perpendicular to the reflecting planes,  $\lambda$  denotes the X-ray wavelength,  $\beta$  denotes the full width at half maximum (FWHM), and  $\theta$  represents the diffraction angle. It is found that the average crystallite domain size of AgNPs was 19 nm which is close to the AgNPs that green synthesized from *Mimosa pudica* leaves extract<sup>32</sup>.

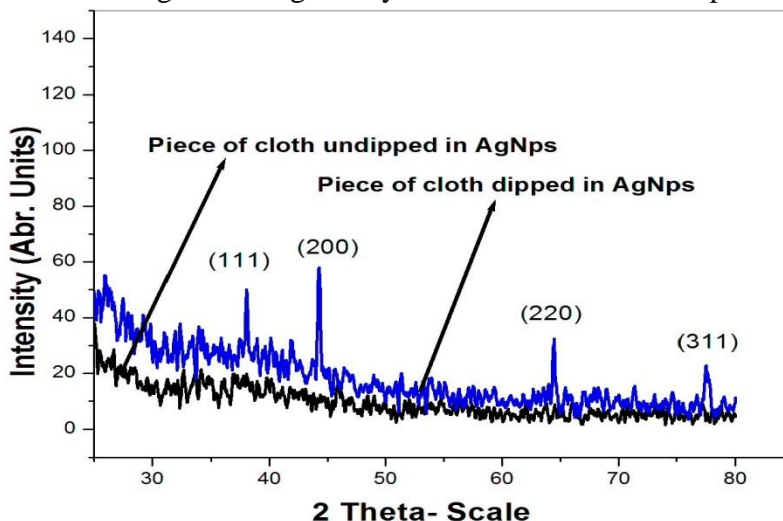


**Figure No 7:** XRD pattern for green synthesized AgNP using microwave-assisted treatment

### Antibacterial activity

#### Disk diffusion antibacterial assay

Inhibition of three types of bacteria, Gram-negative bacteria *E. coli*, Gram-positive bacteria *B. subtilis* and *S. aureus* (the most common infection bacteria in wound) are summarized in Table 1 and illustrated in Fig. 8. The diameter of inhibitory zone ranges from 8 to 14 mm for normal condition and microwave-assisted treatment AgNPs, respectively. The highest inhibitory effect is observed in the treatment with 10  $\mu$ L of 5 mg/mL microwave-assisted treatment AgNPs against *S. aureus*, followed by 10  $\mu$ L of 5 mg/mL normal condition AgNPs against *S. aureus*. It is noticeable that larger inhibitory zones are observed in 10  $\mu$ L of 5 mg/mL microwave-assisted treatment AgNPs for all types of bacteria as compared to 5  $\mu$ L of 5 mg/mL normal condition AgNPs. Furthermore, it is noteworthy that both AgNPs perform better antimicrobial activity against *S. aureus* than *E. coli* and *B. subtilis*<sup>33</sup>. Similar observation was reported by Lomeli-Rosales et al. (2022) with green synthesized AgNPs using leaves extract of *Capsicum chinense*. One possible explanation for higher inhibition against *S. aureus* could be owing to the differences in cell membranes and enzymes present in the periplasmic space. The presence of enzymes allows certain Gram-negative bacteria to degrade externally introduced molecules, as described by Duffy and Power (2001). Additionally, the hydrophilic surface of the bacterial outer membrane is high in lipopolysaccharide molecules, which serves as a barrier for antibiotic penetration, adding to their resistance. Conversely, Gram-positive bacteria do not have an outer membrane or even cell wall structure, making them more susceptible to certain antibacterial agents, according to Shan et al. (2007). This is exemplified by the antimicrobial activity of *Vaccinium bracteatum* Thunb. leaves extract where higher inhibition against *S. aureus* than *E. coli* and *B. subtilis* was demonstrated. Additionally, when comparing both Gram-positive

bacteria, *S. aureus* exhibits larger inhibitory zones than *B. subtilis*. This difference may be attributed to the non-pathogenic nature of *B. subtilis* in environments. These bacteria even have been explored as potential therapeutic agents of negligible consumer risk (Gonzalez et al., 2011). While *B. subtilis* is generally considered harmless and has reported additional probiotic benefits, the specific mechanism of immune stimulation in the intestinal epithelium is still not well-established scientifically. *B. subtilis* spores are a predominant constituent of probiotic formulae and also available as a stand-alone probiotic (Piewngam and Otto, 2020). These properties could potentially explain the slower formation of inhibitory zone for *B. subtilis* compared to *S. aureus*. However, further detailed studies are necessary to elucidate the underlying mechanism behind this phenomenon<sup>34</sup>.

**Table: 1** Disk diffusion antibacterial assay of microwave-assisted treatment AgNP

Volume of AgNPs with normal treatment (5 mg/mL)	Clear Zone (mm)		
	E. Coli	B. Subtilis	S. Aureus
0 $\mu$ L (Control)	No clear zone	No clear zone	No clear zone
5 $\mu$ L	8	9	7
10 $\mu$ L	9	8	11
Amount of AgNPs with microwaveassisted treatment (5 mg/)	Clear Zone (mm)		
	E. Coli	B. Subtilis	S. Aureus
0 $\mu$ L (Control)	No clear zone	No clear zone	No clear zone
5 $\mu$ L	10	9	11
10 $\mu$ L	9	10	13

### Broth antibacterial assay

Broth antibacterial assay is also carried out to determine the minimal concentration of AgNPs with microwave-assisted treatment to inhibit the growth of *E. coli*, *B. subtilis*, and *S. aureus*. The control represents the dry cell weight of bacterial growth in nutrient broth without AgNPs. Results in Table 2 shows that the dry cell weight is reducing with the ncreasing concentration of AgNPs from 20 to 40  $\mu$ g/mL in the nutrient broth. Moreover, there is no growth determined in the 60 and 80  $\mu$ g/mL AgNPs samples. This infers that the minimum inhibitory concentration (MIC) of AgNPs for bacterial growth is 60  $\mu$ g/mL of AgNPs. There are many possible mechanisms proposed to explain the antimicrobial activity of AgNPs. AgNPs could inhibit the action of microorganism by permeating its peptidoglycan layer, interacting with intracellular components such as DNA, ultimately resulting in cellular damage (Hossain et al., 2019). According to Sathishkumar et al. (2009), the interaction of AgNPs with the -SH groups of proteins on the cell walls could potentially block respiration, leading to cell death. In addition, AgNPs may generate reactive oxygen species (ROS), which cause cellular damage and protein leakage. The biosynthesized AgNPs in this study have a very small size (40–150 nm) and large

specific surface area for strong adsorption capacity. Therefore, the antimicrobial activity might perform through the interaction of silver ion on the cell surface by weakening hydrogen bonds<sup>35</sup>.

**Table 2:** Broth antibacterial assay of microwave-assisted treatment AgNPs.

Bacteria Type	concentration of AgNPs (µg/mL)	Weight of Dry Cell (g/L)
<b>E. Coli</b>	0 (control)	0.554 ± 0.011
	15	0.472 ± 0.027
	35	0.061 ± 0.007
	55	0
	75	0
<b>B. subtilis</b>	0 (control)	0.401 ± 0.013
	15	0.498 ± 0.029
	35	0.320 ± 0.011
	55	0
	75	0
<b>S. aureus</b>	0 (control)	0.998 ± 0.041
	15	0.881 ± 0.012
	35	0.093 ± 0.009
	55	0
	75	0

## Conclusion

Using microwave-assisted extraction of pineapple (*Ananas comosus*) leaves with AgNO<sub>3</sub> solution, which is more cheaply, environmentally feasible, and easily accessible, it was successfully established that green synthesis of AgNPs is possible. This method could be appropriate for the quick manufacturing of AgNPs. When compared to standard treatment, the green synthesis of AgNPs was sped up by using microwave-assisted treatment with 20 mM AgNO<sub>3</sub>, 6-8 mL of leaves extract, and 2–6 hours of incubation time. Results of increased SPR intensity with increasing incubation time under UV-Vis spectro-photometry examination provide proof that the green synthesised AgNPs are present. AgNPs were discovered to be hexagonal spherical in shape with a size range between 40 and 150 nm using FE-SEM, which further supported the biosynthesis of AgNPs utilising FTIR and XRD investigations. The minimum inhibitory concentration of silver nanoparticles for bacterial growth is 60 g/mL, and AgNPs also demonstrated antibacterial efficacy against *E. coli*, *B. subtilis*, and *S. aureus*. AgNPs has a stronger capacity to operate as an alternate antiseptic agent, especially in the pharmaceutical industry, and a possible avenue for a variety of applications.

## References

1. Acharya, D., Singha, K.M., Pandey, P., Mohanta, B., Rajkumari, J., Singha, L.P., 2018.

2. Shape dependent physical mutilation and lethal effects of silver nanoparticles on bacteria. *Sci. Rep.* 8 (1), 1–11. <https://doi.org/10.1038/s41598-017-18590-6>.
3. Ahmed, B., Hashmi, A., Khan, M.S., Musarrat, J., 2018. ROS mediated destruction of cell membrane, growth and biofilms of human bacterial pathogens by stable metallic AgNPs functionalized from bell pepper extract and quercetin. *Adv. Powder Technol.* 29 (7), 1601–1616. <https://doi.org/10.1016/j.apt.2018.03.025>.
4. Ahmed, S., Ahmad, M., Swami, B.L., Ikram, S., 2016. A review on plants extract mediated synthesis of silver nanoparticles for antimicrobial applications: a green expertise. *J. Adv. Res.* 7 (1), 17–28.
5. Al-Askar, A.A., Hafez, E.E., Kabeil, S.A., Meghad, A., 2013. Bioproduction of silver-nano particles by *Fusarium oxysporum* and their antimicrobial activity against some plant pathogenic bacteria and fungi. *Life Sci. J.* 10 (3), 2470–2475.
6. Alsamhary, K.I., 2020. Eco-friendly synthesis of silver nanoparticles by *Bacillus subtilis* and their antibacterial activity. *Saudi J. Biol. Sci.* 27 (8), 2185–2191.
7. Arshad, H., Sami, M.A., Sadaf, S., Hassan, U., 2021. *Salvadora persica* mediated synthesis of silver nanoparticles and their antimicrobial efficacy. *Sci. Rep.* 11 (1), 1–11. <https://doi.org/10.1038/s41598-021-85584-w>.
8. Baskaran, X., Vigila, A.V.G., Parimelazhagan, T., Muralidhara-Rao, D., Zhang, S., 2016.
9. Biosynthesis, characterization, and evaluation of bioactivities of leaf extract mediated biocompatible silver nanoparticles from an early tracheophyte, *Pteris tripartita* Sw. *Int. J. Nanomed.* 11, 5789. <https://doi.org/10.2147/IJN.S108208>.
10. Pal N, Mandal S, Shiva K, Kumar B. Pharmacognostical, Phytochemical and Pharmacological Evaluation of *Mallotus philippensis*. *Journal of Drug Delivery and Therapeutics.* 2022 Sep 20;12(5):175-81.
11. Singh A, Mandal S. Ajwain (*Trachyspermum ammi* Linn): A review on Tremendous Herbal Plant with Various Pharmacological Activity. *International Journal of Recent Advances in Multidisciplinary Topics.* 2021 Jun 9;2(6):36-8.
12. Mandal S, Jaiswal V, Sagar MK, Kumar S. Formulation and evaluation of carica papaya nanoemulsion for treatment of dengue and thrombocytopenia. *Plant Arch.* 2021;21:1345-54.
13. Mandal S, Shiva K, Kumar KP, Goel S, Patel RK, Sharma S, Chaudhary R, Bhati A, Pal N, Dixit AK. Ocular drug delivery system (ODDS): Exploration the challenges and approaches to improve ODDS. *Journal of Pharmaceutical and Biological Sciences.* 2021 Jul 1;9(2):88-94.
14. Shiva K, Mandal S, Kumar S. Formulation and evaluation of topical antifungal gel of fluconazole using aloe vera gel. *Int J Sci Res Develop.* 2021;1:187-93.
15. Ali S, Farooqui NA, Ahmad S, Salman M, Mandal S. *Catharanthus roseus* (sadabahar): a brief study on medicinal plant having different pharmacological activities. *Plant Archives.* 2021;21(2):556-9.

16. Mandal S, Jaiswal DV, Shiva K. A review on marketed *Carica papaya* leaf extract (CPLE) supplements for the treatment of dengue fever with thrombocytopenia and its drawback. *International Journal of Pharmaceutical Research*. 2020 Jul;12(3).
17. Mandal S, Vishvakarma P, Verma M, Alam MS, Agrawal A, Mishra A. *Solanum Nigrum* Linn: An Analysis Of The Medicinal Properties Of The Plant. *Journal of Pharmaceutical Negative Results*. 2023 Jan 1:1595-600.
18. Vishvakarma P, Mandal S, Pandey J, Bhatt AK, Banerjee VB, Gupta JK. An Analysis Of The Most Recent Trends In Flavoring Herbal Medicines In Today's Market. *Journal of Pharmaceutical Negative Results*. 2022 Dec 31:9189-98.
19. Mandal S, Vishvakarma P, Mandal S. Future Aspects And Applications Of Nanoemulgel Formulation For Topical Lipophilic Drug Delivery. *European Journal of Molecular & Clinical Medicine*.;10(01):2023.
20. Chawla A, Mandal S, Vishvakarma P, Nile NP, Lokhande VN, Kakad VK, Chawla A. Ultra-Performance Liquid Chromatography (Uplc).
21. Mandal S, Raju D, Namdeo P, Patel A, Bhatt AK, Gupta JK, Haneef M, Vishvakarma P, Sharma UK. Development, characterization, and evaluation of *rosa alba* l extract-loaded phytosomes.
22. Mandal S, Goel S, Saxena M, Gupta P, Kumari J, Kumar P, Kumar M, Kumar R, Shiva K. Screening of *catharanthus roseus* stem extract for anti-ulcer potential in wistar rat.
23. Shiva K, Kaushik A, Irshad M, Sharma G, Mandal S. Evaluation and preparation: herbal gel containing *thuja occidentalis* and *curcuma longa* extracts.
24. Chawalitsakunchai, W., Dittanet, P., Loykulnant, S., Sae-oui, P., Tanpichai, S., Seubsai, A., Prapainainar, P., 2021. Properties of natural rubber reinforced with nano cellulose from pineapple leaf agricultural waste. *Mater. Today Commun.* 28, 102594 <https://doi.org/10.1016/j.mtcomm.2021.102594>.
25. Duffy, C.F., Power, R.F., 2001. Antioxidant and antimicrobial properties of some Chinese plant extracts. *Int. J. Antimicrob. Agents* 17 (6), 527–530.
26. Emeka, E.E., Ojiefoh, O.C., Aleruchi, C., Hassan, L.A., Christiana, O.M., Rebecca, M., Dare, E.O., Temitope, A.E., 2014. Evaluation of antibacterial activities of silver nanoparticles green-synthesized using pineapple leaf (*Ananas comosus*). *Micron* 57,1–5. <https://doi.org/10.1016/j.micron.2013.09.003>.
27. Fatimah, I., Mutiara, N.A.L., 2016. Biosynthesis of silver nanoparticles using *Putri Malu* (*Mimosa pudica*) leaves extract and microwave irradiation method. *Molekul* 11 (2), 288–298. <https://doi.org/10.20884/1.jm.2016.11.2.221>.
28. Galatage, S.T., Hebalkar, A.S., Dhobale, S.V., Mali, O.R., Kumbhar, P.S., Nikade, S.V., Killedar, S.G., 2021. Silver nanoparticles: properties, synthesis, characterization, applications and future trends. *Silver micro-nanoparticles-properties, synthesis, characterization, and applications*. <https://doi.org/10.5772/intechopen.99173>.
29. Gnanasekaran, S., Nordin, N.I.A.A., Jamari, S.S., Shariffuddin, J.H., 2022. Effect of Steam-Alkaline coupled treatment on N36 cultivar pineapple leave fibre for isolation of

- cellulose. *Mater. Today: Proc.* 48, 753–760. <https://doi.org/10.1016/j.matpr.2021.02.216>.
30. Gonzalez, D.J., Haste, N.M., Hollands, A., Fleming, T.C., Hamby, M., Pogliano, K., Nizet, V., Dorrestein, P.C., 2011. Microbial competition between *Bacillus subtilis* and *Staphylococcus aureus* monitored by imaging mass spectrometry. *Microbiology* 157 (9), 2485–2492. <https://doi.org/10.1099/mic.0.048736-0>.
31. Hamdiani, S., Shih, Y.F., 2021. A green method for synthesis of silver-nanoparticles diatomite (AgNPs-D) composite from pineapple (*Ananas comosus*) leaf extract. *Indonesian Journal of Chemistry* 21 (3), 740–752. <https://doi.org/10.22146/ijc.63573>.
32. Hossain, M.M., Polash, S.A., Takikawa, M., Shubhra, R.D., Saha, T., Islam, Z., et al., 2019.
33. Investigation of the antibacterial activity and in vivo cytotoxicity of biogenic silver nanoparticles as potent therapeutics. *Front. Bioeng. Biotechnol.* 7, 239. <https://doi.org/10.3389/fbioe.2019.00239>.
34. Yuet, Y.-L.; Buong, W.-C.; Mitsuaki, N.; Son, R. Synthesis of Silver Nanoparticles by Using Tea Leaf Extract from *Camellia Sinensi*. *Int. J. Nanomed.* **2012**, 7, 4263–4267.
35. Krishnakuma, N.; Adavallan, K. Mulberry leaf extract mediated synthesis of gold nano particles and its anti-bacterial activity against human pathogens. *Adv. Nat. Sci. Nanosci. Nanotechnol.* **2014**, 5, 025018.
36. Jaiswal, S.; Duffy, B.; Jaiswal, A.-K.; Stobie, N.; McHale, P. Enhancement of the antibacterial properties of silver nanoparticles using  $\beta$ -cyclodextrin as a capping agent. *Int. J. Antimicrob. Agents* **2010**, 36, 280–283.
37. Sun, Q.; Cai, X.; Li, J.; Zheng, M.; Chen, Z.; Yu, C.-P. Green synthesis of silver nanoparticles using tea leaf extract and evaluation of their stability and antibacterial activity. *Colloids Surf. Physicochem. Eng. Asp.* **2014**, 444, 226–231.
38. Sajeshkumar, N.-K.; Prem, J.-V.; Jiby, J.-M.; Anupa, S. Synthesis of silver nano particles from curry leaf (*murraya koenigii*) extract and its antibacterial activity. *CIBTech J. Pharm. Sci.* **2015**, 4, 15–25.
39. Awwad, A.-M.; Salem, N.-M. Green synthesis of silver nanoparticles by Mulberry leaves extract. *Nanosci. Nanotechnol.* **2012**, 2, 125–128.
40. Awwad, A.-M.; Salem, N.-M.; Abdeen, A.-O. Biosynthesis of silver nanoparticles using Loquat leaf extract and its antibacterial activity. *Adv. Mater. Lett.* **2013**, 4, 338–342.
41. Shahid, L.; Umer, Y.; Sirajuddin; Kim, W.-C.; Raja, A.-S.; Uddin, M.-K. Proximate Composition and Antioxidant Potential of Leaves from Three Varieties of Mulberry (*Morus* sp.): A Comparative Study. *Int. J. Mol. Sci.* **2012**, 13, 6651–



- 6664.
42. Nuengchamngong, N.; Ingkaninan, K.; Kaewruang, W.; Wongareonwanakij, S.; Hongthongdaeng, B. Quantitative determination of 1-deoxynojirimycin in mulberry leaves using liquid chromatography-tandem mass spectrometry. *J. Pharm. Biomed. Anal.* **2007**, *44*, 853–858.
  43. Bahman, N.; Golboo, M. Influence of Three Morus Species Extracts on  $\alpha$ -Amylase Activity. *Iran. J. Pharm. Res.* **2009**, *8*, 115–119.
  44. Chirino, Y.-I.; Pedraza, C.-J. Role of oxidative and nitrosative stress in cisplatin-induced nephrotoxicity. *Exp. Toxicol. Pathol.* **2009**, *61*, 223–242.
  45. Yang, Y.; Gong, T.; Liu, C.-H.; Chen, R.-Y. Four new 2-arylbenzofuran derivatives from leaves of *Morus alba* L. *Chem. Pharm. Bull.* **2010**, *58*, 257–260.
  46. Kobayashi, Y.; Miyazawa, M.; Kojima, T. The use of *Morus alba* L (mulberry): And *Eucommia ulmoides* (Tochu): Leaves as functional foods: A promising approach in the management of hyperlipidemia. *J. Tradit. Med.* **2010**, *27*, 227–230.
  47. Jagpreet, S.; Navalpreet, S.; Aditi, R.; Deepak, K.; Mohit, R. Facile Approach to Synthesize and Characterization of Silver Nanoparticles by Using Mulberry Leaves Extract in Aqueous Medium and its Application in Antimicrobial Activity. *J. Nanostruct.* **2017**, *7*, 134–140.
  48. Siby, J.; Beena, M. Synthesis of silver nanoparticles by microwave irradiation and investigation of their catalytic activity. *Res. J. Recent Sci.* **2014**, *3*, 185–191.
  49. Dhivya, G.; Rajasimman, M. Synthesis of silver nanoparticles using *Momordica charantia* and its applications. *J. Chem. Pharm. Res.* **2015**, *7*, 107–113.